THE GERONTOLOGICAL SOCIETY OF AMERICA®

Journals of Gerontology: Biological Sciences
cite as: *J Gerontol A Biol Sci Med Sci*, 2020, Vol. 75, No. 4, 621–630
doi:10.1093/gerona/gly256
Advance Access publication November 8, 2018

OXFORD

Original Article

Protective Effects of Ghrelin on Fasting-Induced Muscle Atrophy in Aging Mice

Chia-Shan Wu, PhD,[1,2] Qiong Wei, MD,[2,3] Hongying Wang, MS,[1,4] Da Mi Kim, MS,[1] Miriam Balderas, MD,[5] Guoyao Wu, PhD,[6] John Lawler, PhD,[7] Stephen Safe, PhD,[8] Shaodong Guo, PhD,[1] Sridevi Devaraj, PhD,[5] Zheng Chen, PhD,[9] and Yuxiang Sun, PhD[1,2,*]

[1]Department of Nutrition and Food Science, Texas A&M University, College Station. [2]USDA/ARS Children's Nutrition Research Center, Department of Pediatrics, Baylor College of Medicine, Houston, Texas. [3]Division of Endocrinology, Zhongda Hospital, Southeast University, Nanjing, Jiangsu Province. [4]Laboratory of Lipid and Glucose Metabolism, The First Affiliated Hospital of Chongqing Medical University, China. [5]Department of Pathology and Immunology, Baylor College of Medicine, Houston, Texas. [6]Department of Animal Science, [7]Department of Health and Kinesiology, and [8]Department of Veterinary Physiology and Pharmacology, Texas A&M University, College Station. [9]The University of Texas Health Science Center at Houston.

*Address correspondence to: Yuxiang Sun, PhD, Department of Nutrition and Food Science, Texas A&M University, 214D Cater-Mattil, 2253 TAMU, College Station, TX 77843. E-mail: Yuxiang.Sun@tamu.edu

Received: April 17, 2018; Editorial Decision Date: October 19, 2018

Decision Editor: Rozalyn Anderson, PhD

Abstract

Sarcopenia is the aging-associated progressive loss of skeletal muscle; however, the pathogenic mechanism of sarcopenia is not clear. The orexigenic hormone ghrelin stimulates growth hormone secretion, increases food intake, and promotes adiposity. Here we showed that fasting-induced muscle loss was exacerbated in old ghrelin-null (*Ghrl*$^{-/-}$) mice, exhibiting decreased expression of myogenic regulator *MyoD* and increased expression of protein degradation marker *MuRF1*, as well as altered mitochondrial function. Moreover, acylated ghrelin and unacylated ghrelin treatments significantly increased mitochondrial respiration capacity in muscle C2C12 cells. Consistently, acylated ghrelin and unacylated ghrelin treatments effectively increased myogenic genes and decreased degradation genes in the muscle in fasted old *Ghrl*$^{-/-}$ mice, possibly by stimulating insulin and adenosine monophosphate-activated protein kinase pathways. Furthermore, *Ghrl*$^{-/-}$ mice showed a profile of pro-inflammatory gut microbiota, exhibiting reduced butyrate-producing bacteria *Roseburia* and *ClostridiumXIVb*. Collectively, our results showed that ghrelin has a major role in the maintenance of aging muscle via both muscle-intrinsic and -extrinsic mechanisms. Acylated ghrelin and unacylated ghrelin enhanced muscle anabolism and exerted protective effects for muscle atrophy. Because unacylated ghrelin is devoid of the obesogenic side effect seen with acylated ghrelin, it represents an attractive therapeutic option for sarcopenia.

Keywords: Acyl-ghrelin, Unacylated ghrelin, Sarcopenia, Gut microbiota

Sarcopenia, a degenerative loss of skeletal muscle mass and strength during aging, is a major cause of age-related frailty and disability (1). Given the rising aging population, much effort has been made to develop preventive and therapeutic strategies to mitigate age-associated muscle loss (2). Many pathophysiological and environmental factors, including genetic deficiency, immobility, disuse, endocrine dysfunctions, nutritional deficiencies, and inflammation, have been implicated in age-related skeletal muscle atrophy (3). However, currently the precise mechanisms of sarcopenia are not well defined, and there is no effective therapy without side effects (2).

Ghrelin is a 28-amino acid (AA) peptide hormone produced mainly by the stomach (4) that plays multi-faceted roles in nutritional regulation, metabolism, and inflammation (5). Classically known as the "hunger hormone," ghrelin induces growth hormone (GH) secretion, stimulates food intake, and promotes adiposity via its receptor, the growth hormone secretagogue receptor (GHS-R) (5,6). Ghrelin peptides are found in acylated ghrelin (AG; refers

to the peptide with posttranslational octanoylation at Ser3) and unacylated ghrelin (UAG) forms, with UAG being the predominant form in the circulation (7). AG binds to GHS-R in the nM range, whereas UAG binds to GHS-R at high μM range (8,9). Furthermore, in contrast to AG, UAG does not increase GH release or stimulate food intake (10,11). Ghrelin functions as a nutrient sensor; its levels in the circulation are reflective of energy state, increasing during fasting and decreasing after feeding (12). Interestingly, the decrease in postprandial ghrelin levels depends on the types of macronutrients (12). Because a pharmacological dose of ghrelin is a potent secretagogue of GH that regulates muscle growth and differentiation through the GH–insulin-like growth factor (IGF) axis, ghrelin and ghrelin mimetics have recently emerged as attractive candidates for treating sarcopenia and cachexia (13). Although we and others have reported the beneficial effects of pharmacological doses of ghrelin in treating cachexia and sarcopenia (14–17), the role of endogenous ghrelin in the aging muscle remains undetermined, and the mechanism is unclear.

Accumulating studies indicate that mitochondria have a critical role in maintaining cellular bioenergetics, production of reactive oxygen species, calcium homeostasis, and induction of apoptotic processes; mitochondrial dysfunction is considered a key contributor to the pathophysiology of aging (18,19). Interestingly, *in vitro* studies have shown that AG and UAG promote differentiation and fusion, and inhibit apoptosis of muscle C2C12 cells (20,21). However, whether these effects could be mediated by changes in mitochondrial function is currently unknown.

Skeletal muscle is known to use energy substrates selectively in response to changes in nutrient availability (22,23). Under fed conditions, the insulin signaling pathway is activated in skeletal muscle, resulting in increased AA uptake and enhanced protein synthesis (22). Adenosine monophosphate-activated protein kinase (AMPK), a master regulator of cellular energy metabolism, is very important for protein metabolism (24). During prolonged fasting, the increase in the AMP/ATP ratio or depletion of glycogen stores activates the AMPK and the AMPK pathway in skeletal muscle. Activation of skeletal muscle AMPK-mediated autophagy is important in maintaining muscle integrity and mitochondrial function during prolonged fasting and aging (25). Muscular atrophy is a genetically controlled process involving the activation of the autophagy–lysosome and the ubiquitin–proteasome systems; mitochondrial dysfunction is also known to exacerbate muscular atrophy (26).

Chronic low-grade inflammation is a hallmark of aging (27), and this condition has been suggested to contribute to the loss of muscle mass, strength, and functionality (28). Ghrelin possesses anti-inflammatory properties under a variety of pathological conditions, and administration of exogenous ghrelin attenuates endotoxic shock (29) and experimental colitis (30), and also increases oxidative capacity and reduces triglyceride deposition in the muscles of high-fat diet fed rats (31). Moreover, we recently reported that endogenous ghrelin plays an anti-inflammatory role in diet-induced inflammatory condition (32). When challenged with high fructose corn syrup, ghrelin-null (*Ghrl*$^{-/-}$) mice showed increased adiposity and exacerbated adipose tissue inflammation, indicative of a predisposition toward inflammatory state in *Ghrl*$^{-/-}$ compared to wild-type (WT) mice. Taken together, these findings suggest that, in addition to direct effects on muscle, there may also be extrinsic factors mediating the protective effects of ghrelin. Given the emerging multi-faceted roles of gut microbiota in inflammation, aging, and sarcopenia (33), we investigated the gut microbiota composition in young ghrelin-deficient mice in this study, intended to explore whether microbiome composition at young age may potentially influence muscle health in aging.

In this study, we investigated whether the *Ghrl*$^{-/-}$ mice display increased age-associated muscle wasting, and whether ghrelin-deficient old mice have increased susceptibility to fasting-induced muscle atrophy. Next, we examined the expression profile of mitochondrial genes under fed or fasted conditions *in vivo*, and the effects of AG and UAG on mitochondrial function in muscle C2C12 cells. We then tested whether pharmacological treatment of AG and UAG might protect against fasting-induced muscle atrophy. Finally, we assessed the gut microbiota composition of *Ghrl*$^{-/-}$ mice to explore whether extrinsic mechanism may also contribute to or mediate the effect of ghrelin in muscle.

Methods

Animals

WT and *Ghrl*$^{-/-}$ mice have been fully back-crossed to C57BL/6J background (34). Age-matched male mice were used in this study. In the fed, fasted, and pharmacological studies, 18- to 20-month-old male mice were used, whereas gut microbiome was analyzed in 6-month-old male mice. Animals were housed under controlled temperature and lighting (75 ± 1°F; 12 hour light–dark cycle) with free access to food and water. All diets were from Harlan Teklad (2920X, 16% of calories from fat, 60% from carbohydrates, and 24% from protein). All experiments were approved by the Animal Care Research Committee of the Baylor College of Medicine.

AG and UAG Pharmacological Treatment

AG and UAG were purchased from Phoenix Pharmaceuticals. Fasting-induced atrophy was achieved by 48 hours of food removal (35). Mice were s.c. injected with 500 μg/kg AG or UAG, or with saline solution at time 0 and 24 hours after fasting. At the end of treatment, muscles were collected, weighed, and processed either for RNA extraction or Western blot analysis. In all experiments with subcutaneous injection of AG or UAG, controls were saline-injected animals.

Metabolic Characterizations

Metabolic parameters were measured using an Oxymax open-circuit indirect calorimeter (Columbus Instruments, Columbus, OH). Locomotor activity was measured on x+z-axes using infrared beams to count the number of beam breaks during the recording period. When running wheels were used, the mice had unlimited access to the wheels and were allowed a few days of an adjustment period. Distance run was calculated by multiplying the number of complete rotations by the circumference of the wheel. The diameter of the running wheel was 95 mm. Magnetic Resonance Imaging analysis of body composition was carried out using an EchoMRI Whole Body Composition Analyzer (Echo Medical Systems, Houston, TX). Body composition was measured at time 0, 24, and 48-hour fast.

Cell Culture and Mitochondrial Function Analysis by Seahorse Mito Stress Test

Mouse myoblasts C2C12 cells were obtained from American Type Culture Collection (Manassas, VA) and were maintained in Dulbecco's modified Eagle's medium supplemented with 10% fetal bovine serum and antibiotics (growth medium) at 37°C in an incubator with 5% CO_2. Mitochondria respiration was examined using Seahorse XF Cell Mito Stress Test Kit (Agilent Technologies,

North Billerica, MA, USA) according to manufacturer's instructions. C2C12 cells were seeded in XF 96-well cell culture microplate at 10^3 cells/well density in 200 µL of culture medium. At 24 h after seeding, culture medium was changed to 0.2% fetal bovine serum in Dulbecco's modified Eagle's medium to synchronize the cells. After 16 hours, the synchronized cells were treated with growth medium containing saline, 10 nM or 100 nM AG or UAG for 48 hours, with a change of fresh medium at 24 hours. On the day of mito stress test, assay medium was prepared by supplementing Seahorse XF Base Medium with pyruvate (1 mM), glutamine (2 mM), and glucose (10 mM), adjusted to pH 7.4 with 0.1 N NaOH, followed by sterile filtration. A pre-hydrated sensor cartridge (preloaded with 200 µL of Seahorse XF calibration buffer and placed overnight at 37°C in a non-CO_2 incubator) was loaded with the following reagents that were freshly suspended in assay medium: Oligomycin (20 µL of 10 µM solution) to port A; carbonyl cyanide-4-(trifluoromethoxy) phenylhydrazone (22 µL of 10 µM solution) to port B; Rotenone/Actmycin A (25 µL of 10 µM solution) to port C, and mounted on the analyzer. Concomitantly, a cell culture microplate was removed from 37°C CO_2 incubator, washed twice in assay medium, and incubated in 180 µL assay medium at 37°C in non-CO_2 incubator for 1 hour before the assay. The calibration plate is replaced with the cell culture microplate at the start of the assay program. Data were statistically analyzed after subtraction of non-mitochondrial respiration.

Analysis of Gene Expression

Total RNA was isolated using TRIzol Reagent (Invitrogen, Carlsbad, CA) following the manufacturer's instructions. RNA was treated with DNase and run on gels to validate the purity and quality of the RNA. The complementary DNA was synthesized from 1 µg RNA using the SuperScript III First-Strand Synthesis System for RT-PCR (Invitrogen). Real-time PCR was performed on a Bio-Rad using the SYBR Green PCR Master Mix, according to the protocol provided by the manufacturer. The primers' sequences are available on request. 18S was used as the housekeeping gene.

Western Blotting

Gastrocnemius muscle (GM) tissues were homogenized in RIPA buffer with Complete Protease Inhibitor Cocktail and PhosSTOP phosphatase inhibitor cocktail (Roche Inc., Indianapolis, IN). Protein concentration was measured by the BCA protein assay kit (Pierce, Rockford, IL). Fifty micrograms of proteins from each sample were separated by sodium dodecyl sulfate–polyacrylamide gel electrophoresis, and electro-transferred to nitrocellulose membrane for immunoblot analyses. The following antibodies were used: anti-IRS1 (Cell signaling, 3407S, 1:1000), anti-AMPK (Cell signaling, 2603S, 1:1000), anti-p-AMPK (Thr172; Cell signaling, 2535S, 1:1000), anti-MyoD (Santa Cruz, sc-377460, 1:500), anti-myogenin (Santa Cruz, sc-576, 1:500), anti-GAPDH (Cell signaling, 2118S, 1:1000), anti-rabbit IgG, HRP-linked antibody (Cell signaling, 7074, 1:2000). SignalFire ECL Reagent (Cell signaling, 6883) was used.

AA Analysis by HPLC

Serum samples were used for AA analysis by HPLC, as described previously (36). Concentrations of AAs in samples were quantified based on authentic standards from Sigma Chemicals (St. Louis, MO), using the Waters Millenium-32 workstation.

Gut Microbiota Analysis

Mice were individually housed, and stool was collected in the morning for 3 consecutive days. Nucleic acids were extracted from approximately 0.2 g of stool using the MO BIO PowerSoil extraction kit (MO BIO Laboratories, Carlsbad, CA). Amplification and sequencing of the V4 region of the 16S rRNA gene were performed using the NEXTflex 16S V4 amplicon-Seq Kit 2.0 (Bioo Scientific, Austin, TX) with the following primers: 16S V4 Forward GACGCTCTTCCGATCTTATGGT AATTGTGTGCCAGCMGCCGCGGTAA, and 16S V4 Reverse TGTGCTCTTCCGATCTAGTCAGTCAGCCGGACTA CHVGGGTWTCTAAT. Sequences were generated on the Illumina MiSeq platform (Illumina, San Diego, CA) with a minimum of 800 and an average of 7500 sequences generated per sample. Sequence data were processed as previously described (37). Briefly, sequence data were processed through the LotuS pipeline, and quality filters using the UPARSE algorithm were used to reduce error rates. Taxonomic assignment was performed with RDP as the classifier, and HitDB and SILVA as the selected databases. Alpha diversity was calculated using QIIME 1.7 to generate Chao1 and Shannon diversity index. Beta diversity was determined by the unweighted UniFrac distance and Bray–Curtis dissimilarity. Comparisons between groups were made at various taxonomic levels.

Data Analysis

Data were expressed as means ± SEM. All statistical comparisons in microbiome analysis were calculated within GraphPad prism5 (GraphPad Software, La Jolla, CA) using a two-tailed unpaired *t* test with Welch's corrections. For other data, statistical analysis was performed using unpaired *t* test or analysis of variance. Differences were considered statistically significant at $p < .05$.

Results

Old ghrelin Knockout Mice Showed Increased Adiposity but Reduced Locomotor Activity

To test whether endogenous ghrelin plays a role in age-associated metabolic changes, we examined the metabolic profile of old *Ghrl*$^{-/-}$ and WT mice. Compared to WT mice, 18-month-old *Ghrl*$^{-/-}$ mice showed significant increases in body weight and fat mass (Figure 1A). When normalized to body weight, *Ghrl*$^{-/-}$ mice showed a significant increase in the percentage of fat and a decrease in the percentage of lean mass (Figure 1B). Indirect calorimetry analysis using metabolic chambers showed that, similar to our previous report in 24 weeks of age, young *Ghrl*$^{-/-}$ mice (38), old *Ghrl*$^{-/-}$ mice exhibited similar daily food intake to that of WT mice (Figure 1C). Spontaneous locomotor activity of these mice during light and dark periods was comparable between *Ghrl*$^{-/-}$ and WT mice (Figure 1D). Next, we placed running wheels in the metabolic chambers. Food intake of the WT and *Ghrl*$^{-/-}$ mice remained similar in the presence of running wheels (Figure 1E). Interestingly, the traveled distance on the running wheels was significantly reduced in the old *Ghrl*$^{-/-}$ mice, particularly during the active dark-phase (Figure 1F). Furthermore, total locomotor activity of *Ghrl*$^{-/-}$ mice in the chambers with running wheels was significantly lower than that of the WT mice (Figure 1G). In summary, the metabolic profiling data showed that old *Ghrl*$^{-/-}$ mice had higher body fat, and decreased wheel running distance and locomotor activity.

Ablation of Ghrelin Exacerbated Fasting-Induced Muscle Atrophy

A previous study showed that overexpression of ghrelin in skeletal muscle protects against chemical-induced muscle damage (17). To determine whether endogenous ghrelin is involved in age-associated muscle wasting, we assessed muscle mass and gene expression

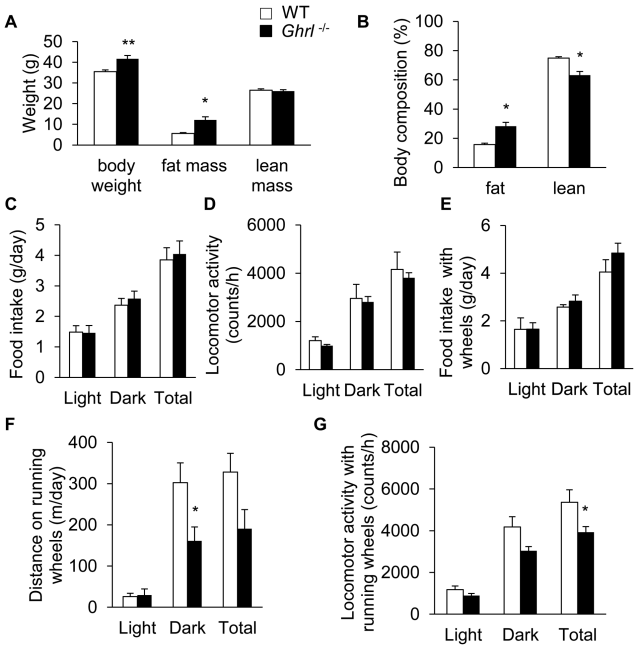

Figure 1. Old ghrelin knockout mice showed increased adiposity and reduced voluntary locomotor activity. Metabolic profiling of wild-type (WT) and *Ghrl*$^{-/-}$ mice at 18 months of age. (**A**) Body weight and composition of the WT and *Ghrl*$^{-/-}$ mice, n = 9–10. (**B**) Body composition of the WT and *Ghrl*$^{-/-}$ mice, normalized to body weight, n = 9–10. (**C**) Daily food intake, n = 6. (**D**) Locomotor activity, n = 6. (**E**) Daily food intake in the presence of running wheels inside metabolic cages, n = 6. (**F**) Total distance run on the running wheels, n = 6. (**G**) Locomotor activity in the presence of running wheels, n = 6. Data are presented as mean ± SEM. *p < .05 versus WT mice, Student's unpaired t test.

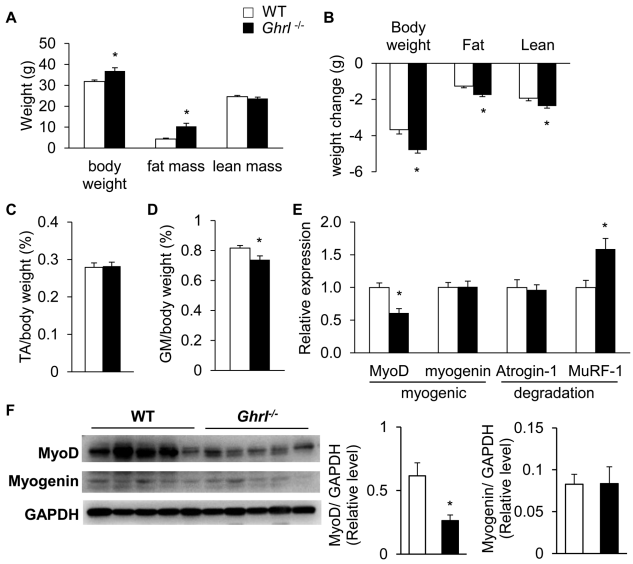

Figure 2. Ablation of ghrelin exacerbated fasting-induced muscle atrophy. Changes of body weight, muscle mass and genes in 20-month-old wild-type (WT) and *Ghrl*$^{-/-}$ mice after 48-hour fasting. (**A**) Body weight and (**B**) body weight change of WT and *Ghrl*$^{-/-}$ mice. (**C**) Percentage of TA depot normalized to body weight. (**D**) Percentage of GM depot, n = 9. (**E**) Relative *MyoD*, *myogenin*, *Atrogin-1*, and *MuRF-1* in GM, n = 4–5. (**F**) Western blots probed for MyoD, Myogenin, and GAPDH proteins, n = 5. Data are presented as mean ± SEM. *p < .05 versus WT mice, Student's unpaired t test.

profiles of old *Ghrl*$^{-/-}$ mice. Gastrocnemius muscle (GM) and tibialis anterior (TA) muscle from fed, 20-month-old WT and *Ghrl*$^{-/-}$ mice were dissected to assess changes in muscle mass. *Ghrl*$^{-/-}$ mice had similar TA and GM mass compared to WT controls (expressed as percent body weight; Supplementary Figures 1A and 1B, respectively). Next, we measured the expression of myogenic regulatory factors, *MyoD* and *myogenin*, and expression of the muscle-specific ubiquitin ligases, *Atrogin-1* and *MuRF1*, which have been reported to drive muscle protein degradation in several models of muscle atrophy (39). We found that under normal fed condition, there was no difference in atrophy gene expression between WT and *Ghrl*$^{-/-}$ mice (Supplementary Figure 1C). Ghrelin is a potent secretagogue of GH (4), often assessed by IGF-1 levels (40), and it has been suggested that expression of *IGF1* in skeletal muscle acts locally in a paracrine/autocrine manner to sustain regeneration in senescent skeletal muscle (41). Similar to our previous report showing that serum IGF-1 levels were not changed in young *Ghrl*$^{-/-}$ mice (38), we did not observe differences in *IGF1* messenger RNA levels in GM of old *Ghrl*$^{-/-}$ mice (Supplementary Figure 1D). Overall, the absence of ghrelin did not alter either the muscle mass or atrophic gene expression in the skeletal muscle of 20-month-old male mice under normal feeding condition.

Next, we used an experimental model of fasting-induced muscle atrophy to assess the role of endogenous ghrelin in muscle atrophy. To induce skeletal muscle atrophy, 20-month-old male WT and *Ghrl*$^{-/-}$ mice were fasted for 48 hours and body weight and body composition were measured (Figure 2A). After 48-hour fasting, old *Ghrl*$^{-/-}$ mice lost significantly more body weight, fat, and lean mass compared to WT mice (Figure 2B). To further investigate the loss of lean mass, we measured the weights of two types of skeletal muscles, TA and GM, which are considered "fast-twitch" glycolytic muscle, predominantly containing IIA and IIB muscle fibers. After a 48-hour fasting, the TA muscle mass (normalized to body weight) was similar in WT and *Ghrl*$^{-/-}$ mice (Figure 2C), whereas GM mass (normalized to body weight) was significantly reduced in *Ghrl*$^{-/-}$ mice compared to WT mice (Figure 2D). Moreover, in this experimental muscle atrophy model, expression of the myogenic regulator *MyoD* was significantly reduced in GM of *Ghrl*$^{-/-}$ mice compared to WT mice, whereas expression of the protein degradation marker *MuRF-1* was significantly increased in GM of *Ghrl*$^{-/-}$ mice compared to WT mice (Figure 2E). We also observed a significant decrease in MyoD protein level in GM of *Ghrl*$^{-/-}$ mice compared to WT, whereas myogenin levels were not significantly different (Figure 2F). Despite the decrease in MyoD levels, the downstream effector cyclin-dependent kinase inhibitor *p21* (42) was increased in the GM of fasted *Ghrl*$^{-/-}$ mice compared to WT mice. Furthermore, the expression of downstream growth phase myogenic genes such as the myosin light chain, phosphorylatable, fast skeletal muscle gene (*Mylpf*), the skeletal muscle alpha-actin gene (*Acta1*), and Troponin I fast skeletal muscle gene (*Tnni2*) (43) was unchanged in the GM of fasted *Ghrl*$^{-/-}$ mice compared to WT mice (Supplementary Figure 2A). Similar to the fed condition, *IGF1* expression in GM was not altered in *Ghrl*$^{-/-}$ mice compared with WT mice under fasted condition (Supplementary Figure 2B).

In addition, we assessed the expression profile of myogenic and degradation markers in the soleus muscle, which contains predominantly "slow-twitch," oxidative type 1 fibers (44). We found no significant difference in the expression of *MyoD*, *Myogenin*, *Atrogin*, *Murf1*, and *p21* between *Ghrl*$^{-/-}$ and WT mice at either fed or fasting state (Supplementary Figure 2C). Interestingly, 48-hour fasting significantly increased expression of *Atrogin* and *Murf1* in the soleus muscle compared to the fed state, regardless of genotype

(Supplementary Figure 2C). This suggested that type 1 oxidative muscles also undergo atrophy under prolonged fasting condition.

AG and UAG Increases Mitochondrial Respiratory Capacity

One of the hallmarks of aging muscle is mitochondrial dysfunction (45,46) and, therefore, we examined the expression of mitochondrial respiratory and biogenesis genes in fed and fasted GM from 20-month-old *Ghrl*$^{-/-}$ and WT mice (Figure 3). We selected the genes involved in mitochondrial function and mitochondrial fusion/fission dynamics based on published works by others (47,48) and our laboratory (49). Expression of NADH dehydrogenase (ubiquinone) 1 beta subcomplex (*Ndufb5*), part of the mitochondrial electron transport chain complex I, was significantly reduced in *Ghrl*$^{-/-}$ mice in the fed state compared to WT mice, but unchanged in the fasting state (Figure 3A). In contrast, expression of ATP synthase-H$^+$ transporting mitochondrial F1 complex beta subunit (*Atp5b*) and mitochondrial malate dehydrogenase (*Mdh2*) was unchanged in *Ghrl*$^{-/-}$ mice compared to WT mice, in either fed or fasting state (Figure 3A). In addition, messenger RNA levels of the mitochondrial fission gene *Drp1* and fusion gene *Mfn2* were both significantly reduced in *Ghrl*$^{-/-}$ mice (Figure 3A), indicating decreased expression of key genes regulating mitochondrial dynamics in the GM of *Ghrl*$^{-/-}$ mice at fed state. In contrast, *Ghrl*$^{-/-}$ mice in the fasting state showed that mitochondrial fission gene *Drp1* was significantly reduced whereas the fusion gene *Mfn2* was significantly induced (Figure 3A). Interestingly, expression of the mitochondrial genes *Ndufb5*, *Atp5b*, *Mdh2*, *Drp1*, *Mfn1*, and *Mfn2* was significantly reduced in the GM under fasted state compared to fed state, regardless of genotype (Figure 3A), suggesting impaired mitochondrial function and dynamics in fasting-induced muscle atrophy condition. Together, these data suggest that mitochondrial function in skeletal muscle is impaired in *Ghrl*$^{-/-}$ mice, exhibiting distinct mitochondrial dynamics between fed versus fasted states.

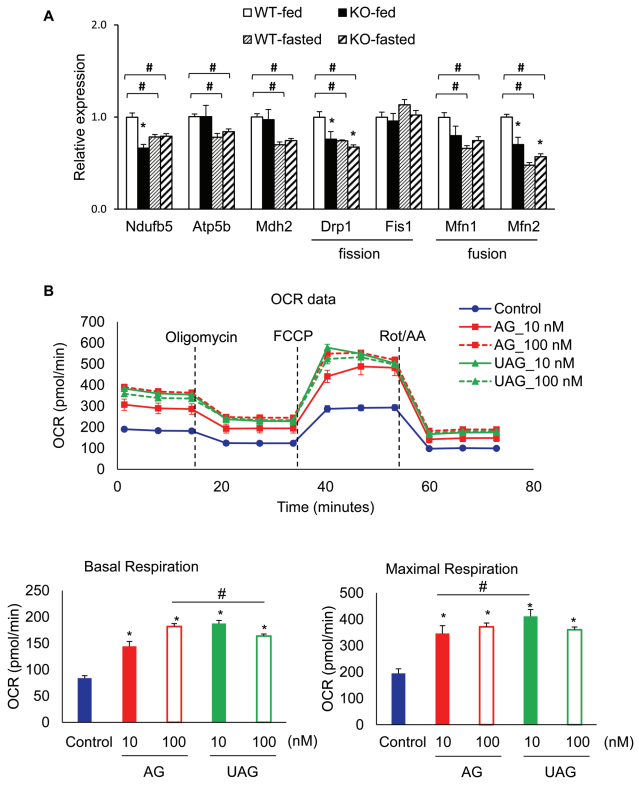

Figure 3. Mitochondrial function in ghrelin-null mice, and acylated ghrelin (AG) and unacylated ghrelin (UAG) treatments on myocyte mitochondrial respiratory function. (**A**) Mitochondrial gene expression changes under fed and fasting condition. Data are presented as mean ± SEM, n = 4–5 per group. The symbol * denotes significant difference to wild-type (WT) mice at either fed or fasting state, and # denotes significant difference to WT-fed state (p < .05 analysis of variance [ANOVA]/Tukey Correction). (**B**) Baseline mitochondrial oxygen consumption rate (OCR), fraction of OCR used for ATP synthesis (determined by mitochondrial OCR after Oligomycin), and respiratory capacity (determined by mitochondrial OCR after addition of the uncoupler carbonyl cyanide-4-(trifluoromethoxy)phenylhydrazone [FCCP]; n = 6). Data are presented as mean ± SEM. *p < .05 versus control, and # denotes significant difference between doses, ANOVA/Tukey Correction.

To further define the role of ghrelin in regulating mitochondrial function, we used *in vitro* mitochondrial respiration assay in C2C12 myoblast cells. Compared to saline control, 48-hour treatment with 10 nM or 100 nM AG dose-dependently increased baseline mitochondrial oxygen consumption rate, and both doses significantly increased maximal oxygen consumption rate (Figure 3B). On the other hand, 48-hour treatment with 10 nM UAG significantly increased baseline and maximal oxygen consumption rate compared to control; however, increasing the dose to 100 nM actually dampened mitochondrial oxygen consumption rate compared to 10 nM dose (Figure 3B).

AG and UAG Treatment Protected Against Fast-Induced Muscle Atrophy in *Ghrl*$^{-/-}$ Mice

To investigate whether pharmacological supplementation with AG and UAG offers protection against fasting-induced muscle atrophy, we injected 20-month-old *Ghrl*$^{-/-}$ mice with saline, AG or UAG before fasting. After 24 hours of fasting, a second dosage of saline, AG, or UAG was injected. After a total of 48-hour fasting, body weight and body composition were measured, mice were killed and weights of TA, GM, and soleus muscles were measured. We found that after 48 hours of treatment with AG or UAG in old *Ghrl*$^{-/-}$ mice did not significantly increase body weight, fat and lean mass, or weights of different types of muscles compared to saline treatment (data not shown). Next, we measured in GM the expression of differentiation and myogenic genes *MyoD* and *myogenin*, and muscle atrophy and degradation genes *Atrogin-1* and *MuRF-1*. AG or UAG significantly increased *MyoD* and *myogenin* expression in GM of *Ghrl*$^{-/-}$ mice, whereas expression of *Atrogin-1* and *MuRF-1* were significantly decreased (Figure 4A). Analysis of protein levels of MyoD showed a trend for increase in AG-treated group but not UAG-treated group compared to saline control (Supplementary Figure 3A). Furthermore, no pronounced differences were observed for *IGF1* gene expression in fasted animals that received saline, AG or UAG treatment (Supplementary Figure 3B). Expression of peroxisome proliferative activated receptor-γ coactivator 1 (*PGC-1α*), a transcription coactivator that stimulates mitochondrial biogenesis and activates AMPK pathway (48), was significantly increased by UAG but not AG treatment (Figure 4B). Furthermore, expression of target myogenic genes downstream of MyoD was significantly increased (*Mylpf*) or showed a trend for increase (*Acta1* and *Tnni2*) by AG or UAG treatment (Figure 4B). Expression of *p21* was unaltered by either AG or UAG treatment (Figure 4B).

A previous study has shown that ghrelin decreases *atrogin* expression in myotubes through increased phosphorylation of Akt in skeletal muscle (17). AMPK also responds to energetic stress to maintain energy

balance in skeletal muscle (25), and recent study showed that muscle regeneration is impaired in AMP-activated protein kinase (*AMPKa1*) knockout mice (50). To explore the downstream signaling pathways mediating the protective effects of AG and UAG in GM, we examined the expression of genes in the insulin signaling pathways (*IRS-1*, *IRS-2*, *Akt*) and *AMPKa1* after treatment with saline, AG or UAG in *Ghrl*$^{-/-}$ mice. In GM of *Ghrl*$^{-/-}$ mice, we found that UAG treatment significantly increased gene expression of *IRS-1* and *IRS-2*, and both AG and UAG significantly increased expression of *AMPKa1* (Figure 4C). At protein levels, there was a trend of increased IRS-1 in AG-treated group, and a trend of increased phosphorylated AMPK (p-AMPK) in both AG- and UAG-treated groups (Figure 4D). Together, these data indicate that acute stimulation with AG and UAG is sufficient to protect *Ghrl*$^{-/-}$ mice from experimentally induced skeletal muscle atrophy, likely through enhancing insulin signaling and activation of AMPK.

AAs are building blocks of muscle, and a number of reports have shown that some AAs are very relevant to muscle atrophy (51). Next, we examined free AA levels in serum of old *Ghrl*$^{-/-}$ mice treated with saline, AG and UAG under 48-hour fasting condition (Supplementary Table 1). Serum arginine levels were significantly reduced in both AG- and UAG-treated mice (Figure 4E), whereas serum taurine and threonine levels were significantly reduced in AG-treated mice only (Figures 4F and 4G). Skeletal muscle is known to express arginase (52). Although the major sites of arginine biosynthesis are the small intestines and kidney, the enzyme arginase drives l-arginine catabolism to l-ornithine, in competition with catabolism to nitric oxide (NO) by NO synthase; this competition has been suggested to limit NO production (53). Interestingly, expression of arginase in GM of *Ghrl*$^{-/-}$ mice was slightly increased by AG and significantly increased by UAG treatments (Figure 4H).

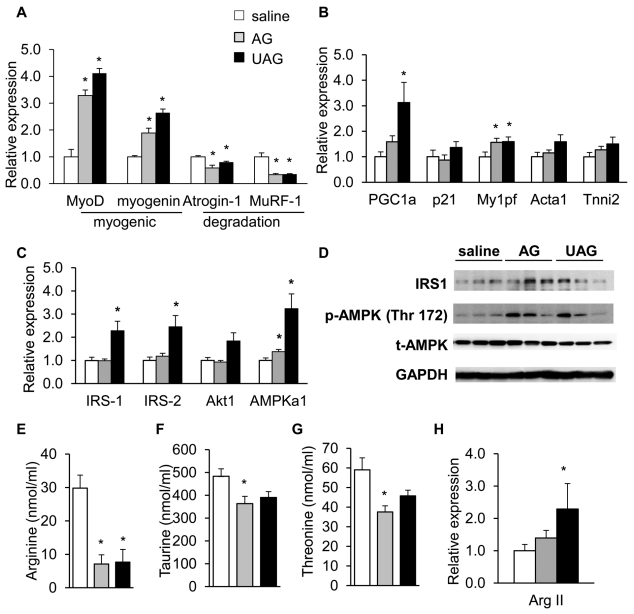

Figure 4. Pharmacological treatment with acylated ghrelin (AG) and unacylated ghrelin (UAG) protected against fasting-induced muscle atrophy in *Ghrl*$^{-/-}$ mice. AG and UAG pharmacological treatment of 20-month-old *Ghrl*$^{-/-}$ mice under 48-hour fasting. (**A**) Relative *MyoD, myogenin, Atroigin-1*, and *MuRF-1* in gastrocnemius muscle (GM), $n = 5$–6. (**B**) Relative *PGC-1α, p21, Mylpf, Acta1, Tnni2* expression in GM, $n = 5$–6. (**C**) Relative expression of genes in insulin signaling pathway (*IRS-1, IRS-2, Akt1*) and *AMPKa1*, $n = 5$–6. (**D**) Western blots probed for IRS-1, p-AMPK, and AMPK proteins, $n = 3$. (**E–G**) Serum from saline, AG- or UAG-treated 20-month-old *Ghrl*$^{-/-}$ mice under 48-hour fasting was analyzed: (**E**) arginine; (**F**) taurine; (**G**) threonine levels, $n = 4$. (**H**) Relative *Arg II* expression in GM, $n = 5$–6. Data are presented as mean ± SEM. *$p < 0.05$ versus saline control, analysis of variance/Bonferroni Correction.

Gut Microbiota Composition Is Shaped by Ghrelin

There is increasing evidence that gut microorganisms and their metabolites influence host responses within the intestinal mucosa as well as the metabolism of host cells in tissues outside the intestine, ultimately modulating energy homeostasis and systemic inflammation (54). To investigate possible alterations in gut microbiota as part of an integrative regulatory mechanism by ghrelin, the variable region 4 (V4) of bacterial 16S ribosomal RNA genes in fecal samples from 6-month-old *Ghrl*$^{-/-}$ and control WT mice were amplified by PCR and sequenced using the Bio Scientific NEXTFlex platform (37). Six-month-old mice were selected to compare microbiome profiles before the divergence of metabolic phenotypes become apparent (34,38). To investigate how ablation of ghrelin affects the microbiota phylogenetic richness in the fecal samples, we analyzed α-diversity as depicted by the Shannon and Chao 1 diversity index (Figures 5A and

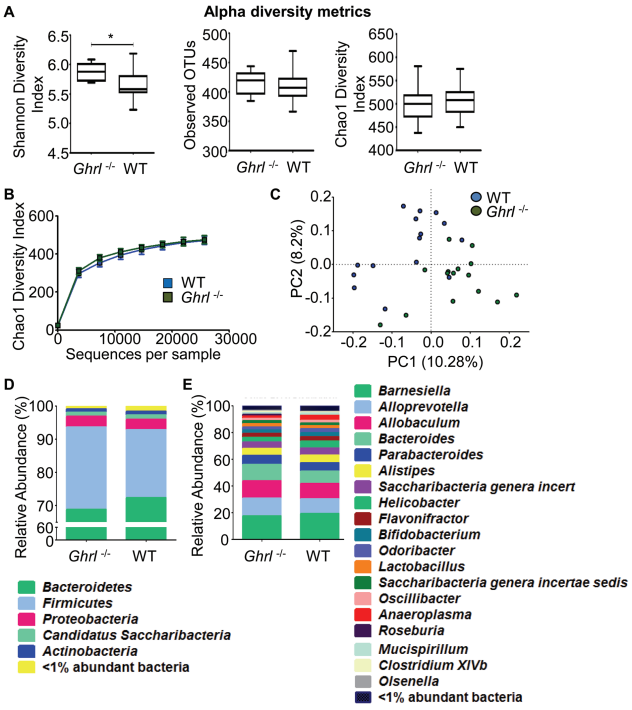

Figure 5. Deletion of ghrelin altered gut microbiota at young age. (**A**) Comparison of alpha diversity metrics for the fecal microbiome of wild-type (WT) and *Ghrl*$^{-/-}$ mice. Shannon diversity index (left panel) reveals a significant variation of microbiota richness and evenness between the intestinal microbiome compositions of the *Ghrl*$^{-/-}$ mice versus WT mice ($p = .003$). No significant differences ($p = .533$) were observed in taxonomic richness across the groups (middle panel) or in the Chao1 diversity index (right panel; $p = .756$). The Chao1 diversity index is another richness estimator that predicts the number of taxa by extrapolating the number of rare organisms. (**B**) Graphical presentation of the Chao1 diversity index. No significant differences were found. (**C**) Beta diversity comparison for the fecal microbiome of WT and *Ghrl*$^{-/-}$ mice. Principal coordinate analysis of mean beta diversity distances (unweighted UniFrac) between all samples. Axes represent two synthetic variables explaining the greatest proportion of variation in the samples. (**D–E**) Taxonomic composition of the fecal microbiome of WT and *Ghrl*$^{-/-}$ mice. Total operational taxonomic unit OTU relative abundances of the two mouse groups is represented at the phylum level (**D**) and the genus level (**E**). Data are presented as mean ± SEM. *$p < .05$ versus WT mice, Student's unpaired *t* test.

5B). Shannon diversity index, a hybrid measure of the richness of a sample and the evenness of taxa in the sample, showed a significant variation of microbiota richness and evenness between the intestinal microbiome composition of the *Ghrl*$^{-/-}$ and WT mice (Figure 5A, far left panel, p = .003). Chao 1 analysis, which predicts the number of taxa in a sample by extrapolating out the number of rare organisms that may have been missed due to under sampling, revealed no significant difference between *Ghrl*$^{-/-}$ and control mice (Chao diversity index, Figures 5A and 5B). We next performed principal coordinate analysis of unweighted UniFrac distances between the fecal samples from *Ghrl*$^{-/-}$ and WT mice, and found that there was a slight separation between the communities (Figure 5C).

Next, taxonomy was assigned to the two groups and represented as "percent abundance" at the level of bacterial phyla (Figure 5D) and genera (Figure 5E). Although no significant differences were detected among the different phyla, there was a trend of decrease in Bacteroidetes and increase in Firmicutes in *Ghrl*$^{-/-}$ mice. Bacteroidetes are associated with healthy lean metabolic state and Firmicutes are associated with obese inflammatory state (55,56). The remainder of the microbiota were composed of divisions commonly encountered at lower abundance in the mouse and human guts: Proteobacteria, Actinobacteria, and *Candidatus Saccharibacteria*. At the genus level, there were decreased *Anaeroplasma* in the *Ghrl*$^{-/-}$ mice in comparison to WT mice (p = .001). However, the amounts of *Roseburia* (= 0.0007) and *ClostridiumXIVb* (p = .025) were significantly decreased in the *Ghrl*$^{-/-}$ mice compared to WT mice. *Roseburia* and *ClostridiumXIVb* are butyrate-producing, gram-positive anaerobic bacteria (57,58), and butyrate protects against high fat diet-induced metabolic changes (59), reduces inflammation (60) and attenuates muscle atrophy during aging (61). Taken together, these data suggest that the composition of gut microbiota in young *Ghrl*$^{-/-}$ has shifted toward a pro-inflammatory state, starting at a young age before metabolic changes are detectable.

Discussion

The loss of muscle mass with aging in sarcopenia is an important contributor to diminished functional ability in the elderly adult (1). Ghrelin, given its role in nutrient sensing and metabolism, is thought logically to be a promising candidate for treating sarcopenia (13). Although several studies have demonstrated the beneficial effects of pharmacological doses of ghrelin in treating cachexia and sarcopenia (14–17), a recent report showed that deletion of ghrelin reduced body weight and preserved muscle function in aging mice (62). Thus, the role of endogenous ghrelin in aging-associated muscle atrophy remains unclear.

Skeletal muscle fibers are broadly classified as "slow-twitch," oxidative (type 1) and "fast-twitch," glycolytic (type 2) muscles (44). Different muscle groups have varying proportions of fiber types, with soleus muscle consisting of predominantly type 1 fibers, and GM consisting of type 2. These proportions of different types of muscle fibers are plastic and display differential susceptibility to various muscle diseases. In particular, sarcopenia and other muscle wasting conditions such as cancer cachexia and fasting have been associated with selective reduction in size and greater atrophy of type 2 fibers (44). Here, we report that old *Ghrl*$^{-/-}$ mice are more susceptible to muscle atrophy under fasting condition, particularly in the GM and not in the soleus muscle, indicating a critical role for endogenous ghrelin in maintaining muscle homeostasis and metabolism in type 2 fibers. Muscle homeostasis is maintained by the anabolic processes of muscle proliferation, differentiation, fusion, and catabolic processes of muscle proteolysis and degradation. MyoD and myogenin belong to a family of proteins known as myogenic regulatory factors, which promote muscle proliferation, differentiation and fusion (43). Atrogin-1 and MuRF-1 are ubiquitin ligases expressed in skeletal muscle that direct the poly-ubiquitination of proteins to target them for proteolysis (39). Here, we showed that, under the fed condition, deletion of ghrelin had no effect on muscle mass and proteolysis in old mice. However, under prolonged fasting, GM of old *Ghrl*$^{-/-}$ mice showed significantly elevated expression of the atrophy gene *MuRF-1*, whereas MyoD, important for muscle differentiation, was reduced at both the gene expression and protein levels. In the state of negative energy (ie, prolonged fasting) muscle wasting occurs through degradation of intracellular macromolecular components via the lysosome-degradation and proteasome systems (63). Because plasma ghrelin increases with fasting (12,64), our data suggest that the endogenous ghrelin is important in maintaining anabolic pathways, especially under nutrient-deficient conditions. This is consistent with the notion that ghrelin is a "thrifty gene," serving as a survival factor under negative energy balance (65).

A key finding from this study is the demonstration of ghrelin's effect on mitochondrial function in aging muscle under atrophic state. Increasing evidence indicate a crucial role for mitochondrial dysfunction in aging-associated degeneration of muscle fibers (18,45,46). Mitochondrial function is impaired in muscle stem cells during aging, manifested in decreased expression of genes involved in electron transport chain as well as decreased oxygen consumption rate in freshly isolated muscle stem cells (47). Furthermore, mitochondrial fusion and fission have emerged as important processes that govern mitochondrial function and contribute to muscle remodeling and atrophy (48,66). Here, we showed that deletion of ghrelin altered mitochondrial function and dynamics in the skeletal muscle of old mice, showing differential function and dynamic changes under fed and fasted conditions. Importantly, *in vitro* analysis of mitochondrial respiratory function in C2C12 cells showed that AG and UAG treatments significantly increased mitochondrial oxygen consumption rates, supporting a cell-autonomous effect of ghrelin on stimulating mitochondrial function in muscle.

Ghrelin peptides are found in acylated (AG) and unacylated (UAG) states in circulation, with UAG being the predominant form (7). Both AG and UAG have been suggested to promote differentiation and fusion and to inhibit apoptosis of muscle C2C12 cells (20,21). In addition, AG and UAG have been shown to protect against atrophy induced by denervation and starvation in WT mice (17). UAG possesses both pro-anabolic and anti-catabolic effects, protecting against burn-induced proteolysis in rodents (67). Here, we used the ghrelin-null mouse model to assess whether pharmacological treatment with AG and UAG could protect the old mice from fasting-induced atrophy. We observed increases in myogenic genes *MyoD*, *Myogenin*, *PGC-1α*, and *Mylpf*, and reduction in atrophy and proteolysis related genes *Atrogin-1* and *MuRF-1*, in both the AG- and UAG-treated groups. These data suggest a shift toward anabolic pathways in the skeletal muscle of AG- and UAG-treated groups. AAs are crucial elements against muscle wasting, and increased protein breakdown is associated with increased AAs in the circulation (51). Indeed, free AA levels in serum showed significant reductions of arginine, threonine, and taurine in the AG-treated group, and reduction of arginine in the UAG-treated group, suggesting reduced proteolysis in GM. Furthermore, arginine can be metabolized in muscle through arginase to ornithine, or through NO synthase to NO (53). The increase in arginase in GM of mice treated with AG and UAG may competitively limit availability of arginine

for the NO production pathway, thus providing an alternative way for protecting against oxidative stress under atrophic condition.

In this study, we did not observe any change in *IGF-1* expression in skeletal muscle of *Ghrl*$^{-/-}$ mice under fed, fasting, or pharmacologically treated conditions. These observations suggest that the GH–IGF-1 axis in *Ghrl*$^{-/-}$ mice is not affected by the absence of ghrelin, nor activated by AG or UAG treatment, consistent with previous reports (17). Importantly, we showed that insulin signaling and activation of AMPK appeared to be increased as a result of AG and UAG treatment, consistent with the increase in myogenic pathways. The increase in insulin signaling by AG and UAG treatment is consistent with previous reports showing anti-atrophic effects of ghrelin in experimentally induced muscle atrophy (17,21). Interestingly, UAG, which is far more abundant in plasma than AG, binds to GHS-R at micromolar concentrations, whereas AG binds to GHS-R at nanomolar concentrations (8,9). Furthermore, UAG regulates gene expression in fat, muscle, and liver independently of GHS-R (11). Here, we showed that UAG at nanomolar concentration can increase mitochondrial oxygen consumption in C2C12 cells, again suggesting the existence of yet unidentified receptor other than GHS-R mediating the anti-atrophic effects of UAG. The corticotropin releasing factor 2 receptor has been suggested to be a receptor for AG in C2C12 cells (68), and may potentially function as a receptor for UAG in myocytes; however, it was reported that corticotropin releasing factor 2 receptor is not a receptor for UAG in INS-1E rat insulinoma cells (69). Hence, the identity of the receptor for UAG remains elusive. Nevertheless, our study supports that similar to AG, UAG has a strong and specific potential for the prevention or treatment of muscle atrophy, while avoiding the adipogenic effects of AG.

Gut microbiota has an important impact on muscle wasting in aging (33), and using our *Ghrl*$^{-/-}$ mouse model we show for the first time that ghrelin plays an important role in regulating gut microbiota. Increased Firmicutes and decreased Bacteroidetes were observed in the gut microflora of young *Ghrl*$^{-/-}$ mice at a time when there was no difference in food intake nor body composition, suggesting that ghrelin inactivation is associated with a pro-inflammatory microbiome profile, similar to microbiome changes observed with the low-grade inflammation resulting from diet-induced obesity and aging (55,56). Moreover, we found a significant reduction in the butyrate-producing bacteria, *Roseburia* and *ClostridiumXIVb*, in the *Ghrl*$^{-/-}$ mice compared to WT mice. Butyrate has been implicated in protection against diet-induced metabolic dysfunctions (59) and exerts anti-inflammatory effects (60). More relevantly, butyrate has been reported to reduce muscle atrophy during aging, likely due to its property as a general histone deacetylase inhibitor (61). The altered microbiome is in line with the increased adiposity and susceptibility to fasting-induced muscle atrophy in old *Ghrl*$^{-/-}$ mice we observed in this study. Previously we reported that *Ghrl*$^{-/-}$ mice exposed to high fructose corn syrup showed exacerbated adipose tissue inflammation and insulin resistance (32). The altered microbiome we detected in *Ghrl*$^{-/-}$ mice may also explain the exacerbated obese and diabetic phenotype of *Ghrl*$^{-/-}$ mice subjected to high fructose corn syrup or sucrose challenge (32). However, more studies are needed to decipher whether there is a direct cause and effect relationship between ghrelin-mediated microbiota changes and muscle mass/function in aging.

Here, we showed that old *Ghrl*$^{-/-}$ mice exhibit increased body weight and adiposity, in contrast to a recent report showing decreased body weight and adiposity in old ghrelin knockout mice (62). This discrepancy may be due to different genetic background of the mice, differences in housing condition and/or rodent diets. Nevertheless, both our study and the other study (62) reported the beneficial effect of AG treatment in improving muscle function. In this study we have used male mice, and the role of endogenous ghrelin in female mice will be investigated in future studies as it is known that sexual dimorphism exists in the muscle transcriptome and muscle mass/strength during aging (70,71).

In summary, our studies demonstrate a key role of ghrelin signaling in maintenance of aged muscle, involving both muscle-intrinsic and -extrinsic mechanisms. We provide *in vivo* evidence that old mice deficient of ghrelin are more susceptible to fasting-induced muscle atrophy, and that AG and UAG can reverse the process by promoting anabolic effect and suppressing catabolic effect in muscle. We report for the first time that the absence of ghrelin shifts the gut microbiota profile toward a pro-inflammatory state, which suggests that ghrelin deficiency may prime the muscle to atrophy as animal ages. Future investigation of the relationship between gut microbiota and muscle function will provide additional insights on the pathogenesis of sarcopenia. AG and UAG hold exciting promise for prevention/treatment of sarcopenia.

Supplementary Material

Supplementary data is are available at *The Journals of Gerontology, Series A: Biological Sciences and Medical Sciences* online.

Funding

This work was supported by American Diabetes Association Award #1-15-BS-177, National Institutes of Health (NIH) R56DK118334, United States Department of Agriculture National Institute of Food and Agriculture Hatch Project 1010840, and Oklahoma Nathan Shock Center of Excellence for the Biology of Aging to Y.S. This work was also partially supported by NIH R01 DK095118 to S.G.; Robert A. Welch Foundation AU-1731 and the National Institute on Aging at NIH R01AG045828 to Z.C. This work was also partially supported by the National Natural Science Foundation of China (Grant No.81401157) to Q.W. Article.

Acknowledgements

Measurements of body composition, food intake, and energy balance were performed in the Mouse Metabolic Research Unit at the U.S. Department of Agriculture/Agricultural Research Service (USDA/ARS) Children's Nutrition Research Center, Baylor College of Medicine, which is supported by funds from the USDA ARS (www.bcm.edu/cnrc/mmru). The authors acknowledge the expert assistance of Mr. Firoz Vohra and the Mouse Metabolic Research Unit (MMRU) Core Director, Dr. Marta Fiorotto. We also thank Mr. Michael R. Honig at Houston's Community Public Radio Station KPFT for his excellent editorial assistance.

Conflict of Interest

The authors declare no competing financial interests.

Reference

1. Marcell TJ. Sarcopenia: causes, consequences, and preventions. *J Gerontol A Biol Sci Med Sci*. 2003;58:M911–M916. doi.org/10.1093/gerona/58.10.M911
2. Campins L, Camps M, Riera A, Pleguezuelos E, Yebenes JC, Serra-Prat M. Oral drugs related with muscle wasting and sarcopenia. A review. *Pharmacology*. 2017;99:1–8. doi:10.1159/000448247
3. Bonaldo P, Sandri M. Cellular and molecular mechanisms of muscle atrophy. *Dis Model Mech*. 2013;6:25–39. doi:10.1242/dmm.010389

4. Kojima M, Hosoda H, Date Y, Nakazato M, Matsuo H, Kangawa K. Ghrelin is a growth-hormone-releasing acylated peptide from stomach. *Nature*. 1999;402:656–660. doi:10.1038/45230
5. Müller TD, Nogueiras R, Andermann ML, et al. Ghrelin. *Mol Metab*. 2015;4:437–460. doi:10.1016/j.molmet.2015.03.005
6. Sun Y, Wang P, Zheng H, Smith RG. Ghrelin stimulation of growth hormone release and appetite is mediated through the growth hormone secretagogue receptor. *Proc Natl Acad Sci U S A*. 2004;101:4679–4684. doi:10.1073/pnas.0305930101
7. Delhanty PJ, Neggers SJ, van der Lely AJ. Des-acyl ghrelin: a metabolically active peptide. *Endocr Dev*. 2013;25:112–121. doi:10.1159/000346059
8. Bednarek MA, Feighner SD, Pong SS, et al. Structure-function studies on the new growth hormone-releasing peptide, ghrelin: minimal sequence of ghrelin necessary for activation of growth hormone secretagogue receptor 1a. *J Med Chem*. 2000;43:4370–4376. doi:10.1021/jm0001727
9. Matsumoto M, Hosoda H, Kitajima Y, et al. Structure-activity relationship of ghrelin: pharmacological study of ghrelin peptides. *Biochem Biophys Res Commun*. 2001;287:142–146. doi:10.1006/bbrc.2001.5553
10. Broglio F, Gottero C, Prodam F, et al. Non-acylated ghrelin counteracts the metabolic but not the neuroendocrine response to acylated ghrelin in humans. *J Clin Endocrinol Metab*. 2004;89:3062–3065. doi:10.1210/jc.2003-031964
11. Delhanty PJ, Sun Y, Visser JA, et al. Unacylated ghrelin rapidly modulates lipogenic and insulin signaling pathway gene expression in metabolically active tissues of GHSR deleted mice. *PLoS One*. 2010;5:e11749. doi:10.1371/journal.pone.0011749
12. Cummings DE, Purnell JQ, Frayo RS, Schmidova K, Wisse BE, Weigle DS. A preprandial rise in plasma ghrelin levels suggests a role in meal initiation in humans. *Diabetes*. 2001;50:1714–1719. doi.org/10.2337/diabetes.50.8.1714
13. Ali S, Garcia JM. Sarcopenia, cachexia and aging: diagnosis, mechanisms and therapeutic options—a mini-review. *Gerontology*. 2014;60:294–305. doi:10.1159/000356760
14. Garcia JM, Cata JP, Dougherty PM, Smith RG. Ghrelin prevents cisplatin-induced mechanical hyperalgesia and cachexia. *Endocrinology*. 2008;149:455–460. doi:10.1210/en.2007-0828
15. Balasubramaniam A, Joshi R, Su C, et al. Ghrelin inhibits skeletal muscle protein breakdown in rats with thermal injury through normalizing elevated expression of E3 ubiquitin ligases MuRF1 and MAFbx. *Am J Physiol Regul Integr Comp Physiol*. 2009;296:R893–R901. doi:10.1152/ajpregu.00015.2008
16. Nagaya N, Uematsu M, Kojima M, et al. Chronic administration of ghrelin improves left ventricular dysfunction and attenuates development of cardiac cachexia in rats with heart failure. *Circulation*. 2001;104:1430–1435. doi:10.1161/hc3601.095575
17. Porporato PE, Filigheddu N, Reano S, et al. Acylated and unacylated ghrelin impair skeletal muscle atrophy in mice. *J Clin Invest*. 2013;123:611–622. doi:10.1172/JCI39920
18. Figueiredo PA, Powers SK, Ferreira RM, Appell HJ, Duarte JA. Aging impairs skeletal muscle mitochondrial bioenergetic function. *J Gerontol A, Biol Sci Med Sci*. 2009;64:21–33. doi:10.1093/gerona/gln048
19. Gonzalez-Freire M, de Cabo R, Bernier M, et al. Reconsidering the role of mitochondria in aging. *J Gerontol A Biol Sci Med Sci*. 2015;70:1334–1342. doi:10.1093/gerona/glv070
20. Filigheddu N, Gnocchi VF, Coscia M, et al. Ghrelin and des-acyl ghrelin promote differentiation and fusion of C2C12 skeletal muscle cells. *Mol Biol Cell*. 2007;18:986–994. doi:10.1091/mbc.e06-05-0402
21. Yu AP, Pei XM, Sin TK, et al. Acylated and unacylated ghrelin inhibit doxorubicin-induced apoptosis in skeletal muscle. *Acta Physiol (Oxf)*. 2014;211:201–213. doi:10.1111/apha.12263
22. Glass DJ. Signalling pathways that mediate skeletal muscle hypertrophy and atrophy. *Nat Cell Biol*. 2003;5:87–90. doi:10.1038/ncb0203-87
23. Kelley DE. Skeletal muscle fat oxidation: timing and flexibility are everything. *J Clin Invest*. 2005;115:1699–1702. doi:10.1172/JCI25758
24. Witczak CA, Sharoff CG, Goodyear LJ. AMP-activated protein kinase in skeletal muscle: from structure and localization to its role as a master regulator of cellular metabolism. *Cell Mol Life Sci*. 2008;65:3737–3755. doi:10.1007/s00018-008-8244-6
25. Bujak AL, Crane JD, Lally JS, et al. AMPK activation of muscle autophagy prevents fasting-induced hypoglycemia and myopathy during aging. *Cell Metab*. 2015;21:883–890. doi:10.1016/j.cmet.2015.05.016
26. de Lange P, Moreno M, Silvestri E, Lombardi A, Goglia F, Lanni A. Fuel economy in food-deprived skeletal muscle: signaling pathways and regulatory mechanisms. *FASEB J*. 2007;21:3431–3441. doi:10.1096/fj.07-8527rev
27. Franceschi C, Campisi J. Chronic inflammation (inflammaging) and its potential contribution to age-associated diseases. *J Gerontol A Biol Sci Med Sci*. 2014;69 (Suppl 1):S4–S9. doi:10.1093/gerona/glu057
28. Dalle S, Rossmeislova L, Koppo K. The role of inflammation in age-related sarcopenia. *Front Physiol*. 2017;8:1045. doi:10.3389/fphys.2017.01045
29. Chang L, Zhao J, Yang J, Zhang Z, Du J, Tang C. Therapeutic effects of ghrelin on endotoxic shock in rats. *Eur J Pharmacol*. 2003;473:171–176. doi.org/10.1016/S0014-2999(03)01972-1
30. Gonzalez-Rey E, Chorny A, Delgado M. Therapeutic action of ghrelin in a mouse model of colitis. *Gastroenterology*. 2006;130:1707–1720. doi:10.1053/j.gastro.2006.01.041
31. Barazzoni R, Zanetti M, Semolic A, et al. High-fat diet with acyl-ghrelin treatment leads to weight gain with low inflammation, high oxidative capacity and normal triglycerides in rat muscle. *PLoS One*. 2011;6:e26224. doi:10.1371/journal.pone.0026224
32. Ma X, Lin L, Yue J, et al. Suppression of ghrelin exacerbates HFCS-induced adiposity and insulin resistance. *Int J Mol Sci*. 2017;18:1302. doi:10.3390/ijms18061302
33. Bindels LB, Delzenne NM. Muscle wasting: the gut microbiota as a new therapeutic target? *Int J Biochem Cell Biol*. 2013;45:2186–2190. doi:10.1016/j.biocel.2013.06.021
34. Ma X, Lin L, Qin G, et al. Ablations of ghrelin and ghrelin receptor exhibit differential metabolic phenotypes and thermogenic capacity during aging. *PLoS One*. 2011;6:e16391. doi:10.1371/journal.pone.0016391
35. Sandri M, Lin J, Handschin C, et al. PGC-1alpha protects skeletal muscle from atrophy by suppressing FoxO3 action and atrophy-specific gene transcription. *Proc Natl Acad Sci U S A*. 2006;103:16260–16265. doi:10.1073/pnas.0607795103
36. Wu G, Davis PK, Flynn NE, Knabe DA, Davidson JT. Endogenous synthesis of arginine plays an important role in maintaining arginine homeostasis in postweaning growing pigs. *J Nutr*. 1997;127:2342–2349. doi:10.1093/jn/127.12.2342
37. Pahwa R, Balderas M, Jialal I, Chen X, Luna RA, Devaraj S. Gut microbiome and inflammation: a study of diabetic inflammasome-knockout mice. *J Diabetes Res*. 2017;2017:6519785. doi:10.1155/2017/6519785
38. Sun Y, Ahmed S, Smith RG. Deletion of ghrelin impairs neither growth nor appetite. *Mol Cell Biol*. 2003;23:7973–7981. doi:10.1128/mcb.23.22.7973-7981.2003
39. Gumucio JP, Mendias CL. Atrogin-1, MuRF-1, and sarcopenia. *Endocrine*. 2013;43:12–21. doi:10.1007/s12020-012-9751-7
40. Juul A, Skakkebaek NE. Prediction of the outcome of growth hormone provocative testing in short children by measurement of serum levels of insulin-like growth factor I and insulin-like growth factor binding protein 3. *J Pediatr*. 1997;130:197–204. doi.org/10.1016/S0022-3476(97)70343-3
41. Musarò A, McCullagh K, Paul A, et al. Localized Igf-1 transgene expression sustains hypertrophy and regeneration in senescent skeletal muscle. *Nat Genet*. 2001;27:195–200. doi:10.1038/84839
42. Zhang P, Wong C, Liu D, Finegold M, Harper JW, Elledge SJ. p21(CIP1) and p57(KIP2) control muscle differentiation at the myogenin step. *Genes Dev*. 1999;13:213–224. doi:10.1101/gad.13.2.213
43. Ishibashi J, Perry RL, Asakura A, Rudnicki MA. MyoD induces myogenic differentiation through cooperation of its NH2- and COOH-terminal regions. *J Cell Biol*. 2005;171:471–482. doi:10.1083/jcb.200502101
44. Talbot J, Maves L. Skeletal muscle fiber type: using insights from muscle developmental biology to dissect targets for susceptibility and resistance to muscle disease. *Wiley Interdiscip Rev Dev Biol*. 2016;5:518–534. doi:10.1002/wdev.230

45. Johnson ML, Robinson MM, Nair KS. Skeletal muscle aging and the mitochondrion. *Trends Endocrinol Metab*. 2013;24:247–256. doi:10.1016/j.tem.2012.12.003
46. Zhang X, Trevino MB, Wang M, et al. Impaired mitochondrial energetics characterize poor early recovery of muscle mass following hind limb unloading in old mice. *J Gerontol A Biol Sci Med Sci*. 2018;73:1313–1322. doi:10.1093/gerona/gly051
47. Zhang H, Ryu D, Wu Y, et al. NAD+ repletion improves mitochondrial and stem cell function and enhances life span in mice. *Science*. 2016;352:1436–1443. doi:10.1126/science.aaf2693
48. Cannavino J, Brocca L, Sandri M, Grassi B, Bottinelli R, Pellegrino MA. The role of alterations in mitochondrial dynamics and PGC-1α overexpression in fast muscle atrophy following hindlimb unloading. *J Physiol*. 2015;593:1981–1995. doi:10.1113/jphysiol.2014.286740
49. Lin L, Lee JH, Bongmba OY, et al. The suppression of ghrelin signaling mitigates age-associated thermogenic impairment. *Aging (Albany NY)*. 2014;6:1019–1032. doi:10.18632/aging.100706
50. Mounier R, Théret M, Arnold L, et al. AMPKα1 regulates macrophage skewing at the time of resolution of inflammation during skeletal muscle regeneration. *Cell Metab*. 2013;18:251–264. doi:10.1016/j.cmet.2013.06.017
51. Wandrag L, Brett SJ, Frost G, Hickson M. Impact of supplementation with amino acids or their metabolites on muscle wasting in patients with critical illness or other muscle wasting illness: a systematic review. *J Hum Nutr Diet*. 2015;28:313–330. doi:10.1111/jhn.12238
52. Pardridge WM, Duducgian-Vartavarian L, Casanello-Ertl D, Jones MR, Kopple JD. Arginine metabolism and urea synthesis in cultured rat skeletal muscle cells. *Am J Physiol*. 1982;242:E87–E92. doi:10.1152/ajpendo.1982.242.2.E87
53. Wu G, Morris SM, Jr. Arginine metabolism: nitric oxide and beyond. *Biochem J*. 1998;336 (Pt 1):1–17. doi: 10.1042/bj3360001
54. Delzenne NM, Cani PD. Interaction between obesity and the gut microbiota: relevance in nutrition. *Annu Rev Nutr*. 2011;31:15–31. doi:10.1146/annurev-nutr-072610-145146
55. Devaraj S, Hemarajata P, Versalovic J. The human gut microbiome and body metabolism: implications for obesity and diabetes. *Clin Chem*. 2013;59:617–628. doi:10.1373/clinchem.2012.187617
56. Boulangé CL, Neves AL, Chilloux J, Nicholson JK, Dumas ME. Impact of the gut microbiota on inflammation, obesity, and metabolic disease. *Genome Med*. 2016;8:42. doi:10.1186/s13073-016-0303-2
57. Tamanai-Shacoori Z, Smida I, Bousarghin L, et al. Roseburia spp.: a marker of health? *Future Microbiol*. 2017;12:157–170. doi:10.2217/fmb-2016-0130
58. Lopetuso LR, Scaldaferri F, Petito V, Gasbarrini A. Commensal clostridia: leading players in the maintenance of gut homeostasis. *Gut Pathog*. 2013;5:23. doi:10.1186/1757-4749-5-23
59. Gao Z, Yin J, Zhang J, et al. Butyrate improves insulin sensitivity and increases energy expenditure in mice. *Diabetes*. 2009;58:1509–1517. doi:10.2337/db08-1637
60. Maslowski KM, Vieira AT, Ng A, et al. Regulation of inflammatory responses by gut microbiota and chemoattractant receptor GPR43. *Nature*. 2009;461:1282–1286. doi:10.1038/nature08530
61. Walsh ME, Bhattacharya A, Sataranatarajan K, et al. The histone deacetylase inhibitor butyrate improves metabolism and reduces muscle atrophy during aging. *Aging Cell*. 2015;14:957–970. doi:10.1111/acel.12387
62. Guillory B, Chen JA, Patel S, et al. Deletion of ghrelin prevents aging-associated obesity and muscle dysfunction without affecting longevity. *Aging Cell*. 2017;16:859–869. doi:10.1111/acel.12618
63. Sandri M, Coletto L, Grumati P, Bonaldo P. Misregulation of autophagy and protein degradation systems in myopathies and muscular dystrophies. *J Cell Sci*. 2013;126:5325–5333. doi:10.1242/jcs.114041
64. Tschöp M, Wawarta R, Riepl RL, et al. Post-prandial decrease of circulating human ghrelin levels. *J Endocrinol Invest*. 2001;24:RC19–RC21. doi:10.1007/BF03351037
65. Zhang Y, Fang F, Goldstein JL, Brown MS, Zhao TJ. Reduced autophagy in livers of fasted, fat-depleted, ghrelin-deficient mice: reversal by growth hormone. *Proc Natl Acad Sci U S A*. 2015;112:1226–1231. doi:10.1073/pnas.1423643112
66. Romanello V, Guadagnin E, Gomes L, et al. Mitochondrial fission and remodelling contributes to muscle atrophy. *EMBO J*. 2010;29:1774–1785. doi:10.1038/emboj.2010.60
67. Sheriff S, Kadeer N, Joshi R, Friend LA, James JH, Balasubramaniam A. Des-acyl ghrelin exhibits pro-anabolic and anti-catabolic effects on C2C12 myotubes exposed to cytokines and reduces burn-induced muscle proteolysis in rats. *Mol Cell Endocrinol*. 2012;351:286–295. doi:10.1016/j.mce.2011.12.021
68. Gershon E, Vale WW. CRF type 2 receptors mediate the metabolic effects of ghrelin in C2C12 cells. *Obesity (Silver Spring)*. 2014;22:380–389. doi:10.1002/oby.20535
69. Gauna C, Delhanty PJ, van Aken MO, et al. Unacylated ghrelin is active on the INS-1E rat insulinoma cell line independently of the growth hormone secretagogue receptor type 1a and the corticotropin releasing factor 2 receptor. *Mol Cell Endocrinol*. 2006;251:103–111. doi:10.1016/j.mce.2006.03.040
70. Liu D, Sartor MA, Nader GA, et al. Microarray analysis reveals novel features of the muscle aging process in men and women. *J Gerontol A Biol Sci Med Sci*. 2013;68:1035–1044. doi:10.1093/gerona/glt015
71. Kim KM, Lim S, Oh TJ, et al. Longitudinal changes in muscle mass and strength, and bone mass in older adults: gender-specific associations between muscle and bone losses. *J Gerontol A Biol Sci Med Sci*. 2018;73:1062–1069. doi:10.1093/gerona/glx188